Title	An Efficient Method for Estimation of Reduction of Welding Residual Stresses from Stress-Relief Annealing (Report IV) : Applicability of the Method for Stress-Relief Annealing of Thick Welded Joints(Mechanics, Strength & Structure Design)
Author(s)	Nakacho, Keiji; Ueda, Yukio
Citation	Transactions of JWRI. 1996, 25(1), p. 101-108
Version Type	VoR
URL	https://doi.org/10.18910/12528
rights	
Note	

An Efficient Method for Estimation of Reduction of Welding Residual Stresses from Stress-Relief Annealing (Report IV) †

- Applicability of the Method for Stress-Relief Annealing of Thick Welded Joints -

Keiji NAKACHO* and Yukio UEDA**

Abstract

Stress-relief annealing (SR treatment) is included in the fabrication process of welded structures such as pressure vessels. This study aims to develop a simple analytical method to facilitate the calculation of transient and residual stresses during SR treatment, in order to easily determine the reasonable conditions for SR treatment of recent large-size structures of high-quality thick plates.

In the first report, estimation equations for uni-axial stress state were formulated for relaxation tests at changing and constant temperatures. In the second report, the stresses relaxed by SR treatments in thick welded joints were analyzed accurately by the finite element method based on thermal elastic-plastic creep theory. The characteristics of the changes in the welding residual stresses in multi-axial stress states were studied in detail. In the third report, estimation equations for multi-axial stress state were developed for thick welded joints, based on the above characteristics. In this report, the stress relaxation phenomena of thick welded joints during SR treatment are analyzed by applying the estimation equations. The accuracy of the method is investigated, comparing the results with ones by FEM.

KEY WORDS : (Simple Estimation Method) (Stress-Relief Annealing) (Welding) (Thick Welded Joint) (Transient Stress) (Residual Stress) (Thermal Elastic-Plastic Creep Analysis)

1. Introduction

Stress-relief annealing (hereinafter called SR treatment), whose main purpose is to relieve welding residual stresses, is included in the fabrication process of welded structures such as pressure vessels. Standard conditions for SR treatment are specified in JIS, ASME code, etc. For recent large-size structures constructed of high-quality thick plates, the specified conditions require keeping the structures at a high temperature, near 700 °C, for a long time in proportion to the thickness. Repeating this treatment in the fabrication and repair processes may degrade the qualities of the steel and the joint. The main reason for the difficulty in specifying rational conditions for SR treatment is that the real effect of SR treatment on stress relief (that is, the real change of welding residual stress during SR treatment) is not fully known, especially for thick joints. So more severe conditions for SR treatment are specified for safety from the viewpoint of residual stress.

On the other hand, the available theory [1), 2)] of thermal elastic-plastic creep analysis based on the finite element method had been developed, and with this theory, the changes of stresses in the welded joint of a very thick plate due to SR treatment have been computed [2)]. However, the theory and computer program for analysis are so complicated that it is not easy to perform the analysis. Furthermore, for the three-dimensional problem, very long CPU time is necessary for computation even with a super-computer. Each analyzed result does not always have the essentials of the behavior or the mechanism.

This study aims to develop a simple analytical method (as simple as hand calculation) to facilitate the calculation of transient and residual stresses during SR treatment in order to determine easily the reasonable conditions for SR treatment by parametric study. For this purpose, some relations between stresses and strains during SR

---

† Received on July 5, 1996

* Assistant Professor

** Emeritus Professor

treatment are idealized, and estimation equations are developed.

In the first report [3], estimation equations for the uni-axial stress state were formulated for relaxation tests at changing and constant temperatures, which present phenomena similar to the stress relaxation during SR treatment. It was shown that the analytical results by simple calculations using these equations are highly accurate.

In the second report [4], the stresses relaxed by SR treatment in thick welded joints were analyzed accurately by the finite element method based on thermal elastic-plastic creep theory. The characteristics of the changes of the welding residual stresses in the multi-axial stress state were studied in detail.

In the third report [5], the simple analytical method for the uni-axial stress state, shown in the first report, was expanded and applied to the multi-axial stress state. The characteristics of stress relaxation phenomena in SR treatment of thick welded joints, obtained in the second study, were then utilized. As a result, estimation equations were developed, which could calculate the changes of welding residual stresses during SR treatment in thick welded joints.

In this report, the applicability of the method is investigated. The stress relaxation phenomena in thick welded joints during SR treatment are analyzed by applying the estimation equations developed in the third study. The results are compared with the accurate ones obtained by FEM in the second study.

2. Accurate Analysis by Finite Element Method [4]

The stresses relaxed by SR treatment in thick welded joints were analyzed accurately by the finite element method in the second study. In this chapter, the conditions and the results of these analyses are summarized.

2.1 Specimen and Process of Welding

The specimen in this serial study is shown in **Fig. 1**. Two long plates of 100 mm thickness and 195 mm width are welded with a 10 mm groove width by multi-pass welding. The welding method is narrow gap arc welding. The welding starts from the bottom and finishes with 20 passes and 20 layers. After the welding, stress-relief annealing is performed.

The material of the specimen is ASTM A336F22 (2 1/4 Cr - 1 Mo steel), and the wire is US521AxMF29A (made by Kobe Steel, Ltd.). Their physical, mechanical and creep properties are indicated in the second report. The mechanical properties change depending on the history of temperature. The creep properties change depending on the temperature, that is, below 575 °C or above 575 °C. These material properties are used in the analyses by the FEM and the simple estimation method of this study.

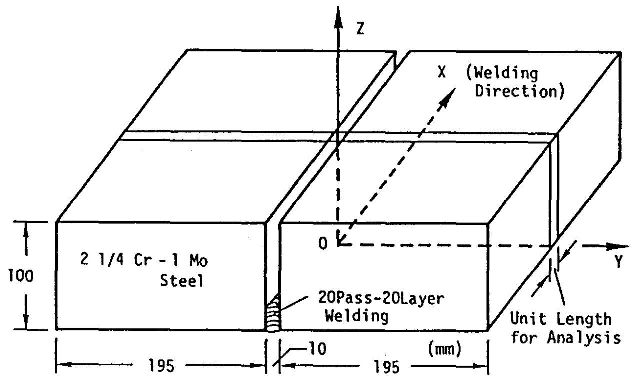

Fig. 1 Specimen of thick welded joint for analysis

2.2 Conditions of Welding and Stress-Relief Annealing

The welding conditions are the same for all welding passes. The heat input is 35,000 J/cm, and the heat efficiency is 0.9. The preheating and inter-pass temperatures are 200 °C.

The conditions of stress-relief annealing for the welded specimen are as follows. The heating rate is slow, that is, 30 °C/hr, because of the large thickness of the joint. The maximum heating temperature is 650 °C, and at that temperature the specimen is held for 1 hour.

2.3 Method of Analysis

It is considered in this study that the specimen is sufficiently long and the welding speed is sufficiently fast. In such a case, it is rational to assume that any YZ-plane in the specimen, except near both ends, is allowed to move, remaining as a flat plane (plane deformation). In this study, a three-dimensional stress analysis is performed, based on this assumption, in thermal elastic-plastic-creep analysis.

The welding stresses in the specimen and their changes during SR treatment were analyzed continuously. The thermal elastic-plastic creep analyses were performed by applying the finite element method whose theory had been developed by the authors [1), 2)]. The analysis as a plane deformation needs only the same memory capacity and CPU time as a two-dimensional analysis.

2.4 Restraint Conditions of Specimen

As the restraint conditions of the specimen, two versions were adopted as shown in **Figs. 2 (a) and (b)**. In restraint condition A, no external restraint is loaded on the specimen during welding and SR treatment. In restraint condition B, longitudinal bending deformation (rotation around Y-axis) and angular distortion (rotation around X-axis) are restricted. In both restraint conditions, the displacement in the direction of plate width (along Y-axis) can occur. These restraint conditions are the opposite extreme restraint conditions for an actual butt joint.

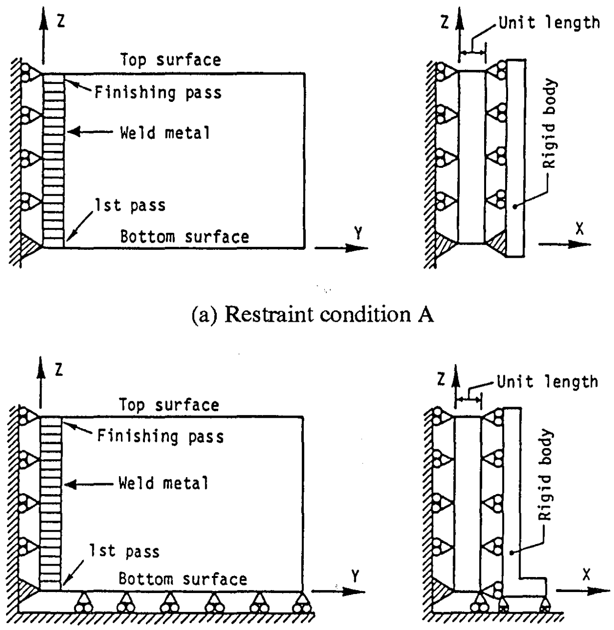

(a) Restraint condition A

(a) Restraint condition B

Fig. 2 Restraint conditions of specimen

2.5 Analytical Results

The results obtained by the thermal elastic-plastic creep analyses are shown in **Figs. 3 and 4**, which are the transient and residual distributions of longitudinal (in the direction of welding) stress σ_x and transverse (in the direction of plate width) stress σ_y during welding and SR treatment. Figure 3 is in the case of the restraint condition A. Figure 4 is in the case B. Figures (a) represent the distributions at the middle cross section (Y=0) and Figs. (b) represent those on the top surface (Z=100 mm), respectively.

The maximum tensile stress is most important in relation to the various cracks, so attention has to be focused on its value and position. The maximum tensile stress is σ_x component, and it appears a little inside of the top surface at the middle cross section, that is, at the point A in Figs. (a). On the surface, the maximum σ_x is produced at the toe of weld, that is, at the point B in Figs (b).

3. Estimation Equations and Method for Multi-Axial Stress States in Thick Welded Joints [5]

The estimation equations for multi-axial stress states in thick welded joints were developed in the third study, based on the characteristics of the phenomenon. In this chapter, the estimation equations and the calculation procedures are summarized.

3.1 Estimation Equations

The equations (18) - (22) in the third report are used for the estimation of the stress change. They are shown below, as Eqs. (1) - (5). (For the details of notations, refer to the third report.)

3.1.1 Heating Stage

(a) In the temperature range below 575 °C (In obedience to strain-hardening theory)

$$m\int_{T_{ss}}^{T_{es}} A^{1/m} E^{\gamma/m}\, dT = -C_s v (\varepsilon^e_{x10s})^{(1-\gamma)/m} \times \int_1^{{}_n\varepsilon^e_{x1}} ({}_n\varepsilon^e_{x1})^{-\gamma/m} (1-{}_n\varepsilon^e_{x1})^{(1/m)-1}\, d\,{}_n\varepsilon^e_{x1} \qquad (1)$$

Where

$$C_s = C_{ss} C_{sb}$$
$$C_{ss} = (2/3) S_1^{1-(\gamma/m)} S_2^{-1} S_3^{(1/m)-1} S_4^{-1/m} \qquad (2)$$
$$C_{sb} = b_1^{1/m}$$

${}_n\varepsilon^e_{x1}$: Normalized equivalent elastic strain

$${}_n\varepsilon^e_{x1} = \varepsilon^e_{x1} / \varepsilon^e_{x10s}$$

(b) In the temperature range above 575 °C (In obedience to power theory)

$$\int_{T_{sp}}^{T_{ep}} \beta E^n\, dT = -C_p \frac{v}{1-n} \{(\varepsilon^e_{x1})^{1-n} - (\varepsilon^e_{x10p})^{1-n}\} \qquad (3)$$

Where

$$C_p = C_{ps} C_{pb}$$
$$C_{ps} = (2/3) S_1^{1-n} S_2^{-1} S_4^{-1} \qquad (4)$$
$$C_{pb} = b_1$$

3.1.2 Holding Stage

$$\varepsilon^{e}_{x1} = \left\{ (\varepsilon^{e}_{x10pc})^{1-n} + C_p^{-1} (n-1) \beta E^{n} t \right\}^{1/(1-n)} \tag{5}$$

Where ε^{e}_{x10pc} : Initial value of ε^{e}_{x1} in the holding stage
t : Time after start of holding (min)

3.2 Calculation Procedure and Tables of Integrations

The stress change during SR treatment can be obtained with Eqs. (1)-(5). The calculation procedure is shown in **Fig. 5**. Three integrations are included in Eqs. (1) and (3). **Tables 1, 2 and 3** are the results of the integrations, and they can be utilized in the calculation. It makes the calculation simpler.

Coefficients C_s and C_p in Eqs. (1)-(4) consist of coefficients S_1 ~ S_4, b_1 and creep constants m, γ and n. For creep constants m, γ and n, the values at the mean temperature in each integration range are used as in the preparation of the three tables mentioned above. Coefficients S_1 ~ S_4 (Eq. (8) in the third report) are shown as follows, and they are assumed to be calculated from the initial stresses in SR treatment, namely, the welding residual stresses.

$$^{E}\sigma = S_1 \sigma_x, \quad ^{d}\sigma_x = S_2 \sigma_x, \quad ^{E}\varepsilon^{c} = S_3 \varepsilon^{c}_{x}, \quad \sigma_x = S_4 E \varepsilon^{e}_{x} \tag{6}$$

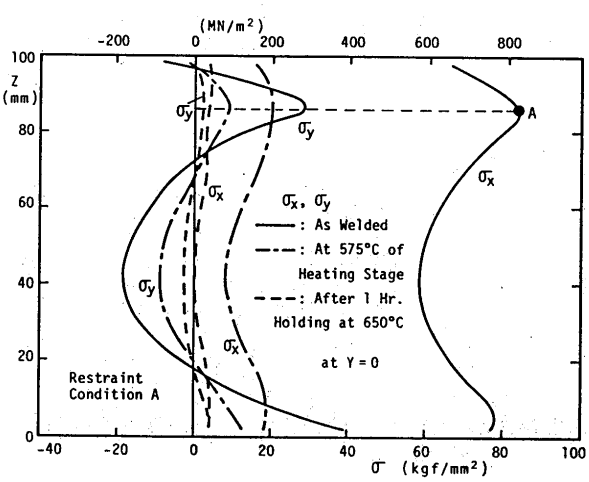

(a) At the middle cross-section (Y = 0)

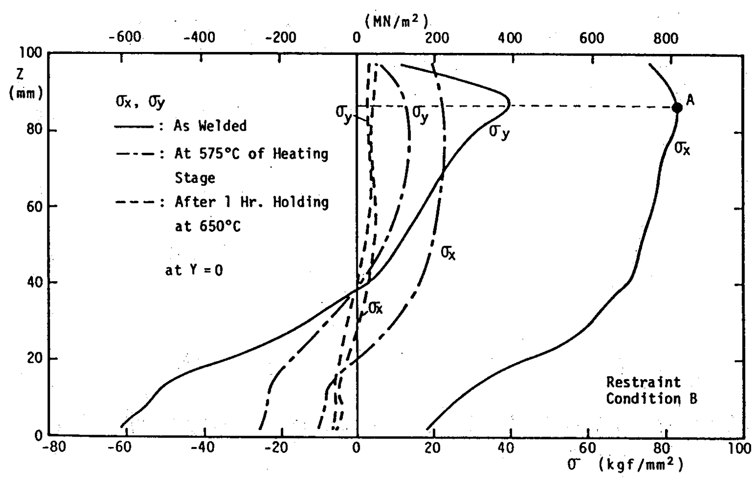

(a) At the middle cross-section (Y = 0)

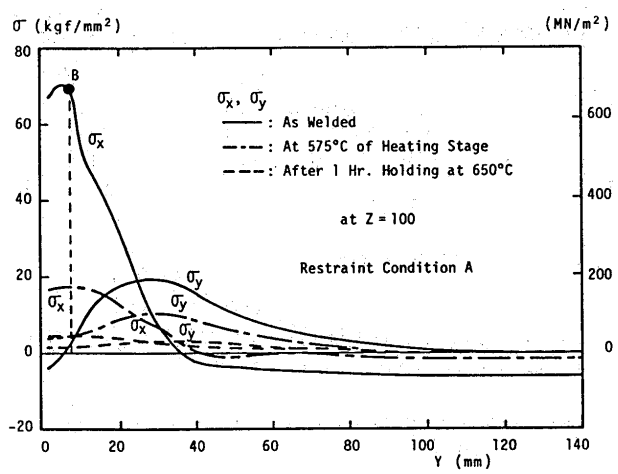

(b) On the top surface (Z = 100 mm)

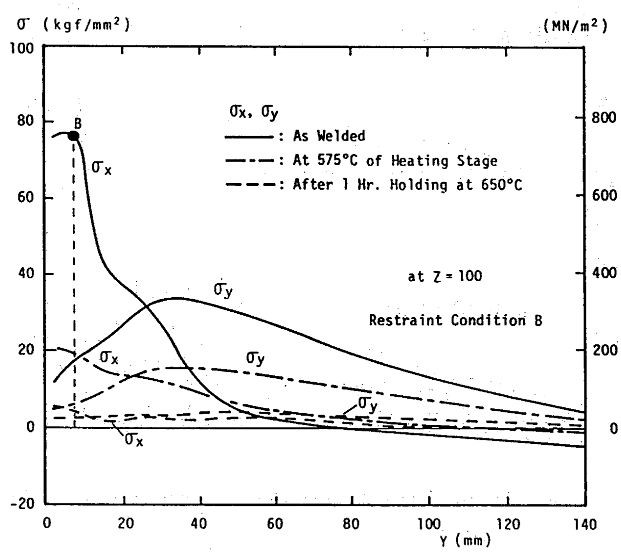

(b) On the top surface (Z = 100 mm)

Fig. 3 Longitudinal and transverse stresses in thick welded joint after welding and during SR
(In the case of restraint condition A)

Fig. 4 Longitudinal and transverse stresses in thick welded joint after welding and during SR
(In the case of restraint condition B)

A. For Strain-Hardening Creep Theory

Eq. (1) may be expressed as

$$-C_s^{-1}(m/v)\,(\varepsilon^e_{x10s})^{(\gamma-1)/m}\cdot I_{ps} = I_s$$

where

$$I_{ps} \equiv \int_{T_{ss}}^{T_{es}} A(T)^{1/m}\,E(T)^{\gamma/m}\,dT, \quad I_s \equiv \int_1^{{}_n\varepsilon^e_{x1}} ({}_n\varepsilon^e_{x1})^{-\gamma/m}\,(1-{}_n\varepsilon^e_{x1})^{(1/m)-1}\,d_n\varepsilon^e_{x1}$$

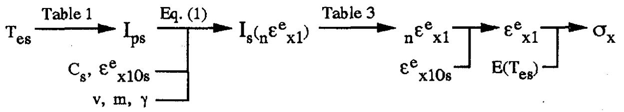

B. For Power Creep Theory

B - 1 At the heating stage

Eq. (3) may be expressed as

$$-C_p^{-1}(1-n)/v\cdot I_{pp} + (\varepsilon^e_{x10p})^{1-n} = (\varepsilon^e_{x1})^{1-n}$$

where

$$I_{pp} \equiv \int_{T_{sp}}^{T_{ep}} \beta(T)\,E(T)^n\,dT$$

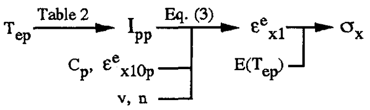

B - 2 At the holding stage

Eq. (5) is expressed as

$$\varepsilon^e_{x1} = \{(\varepsilon^e_{x10pc})^{1-n} + C_p^{-1}(n-1)\,\beta\,E^n\,t\}^{1/(1-n)}$$

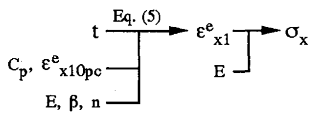

Fig. 5 Flowchart of calculations by simple estimation method

T_{es}	I_{ps}	T_{es}	I_{ps}	T_{es}	I_{ps}
401	1.2884E+15	461	3.1953E+18	521	6.7715E+20
403	4.2382E+15	463	3.8227E+18	523	8.0926E+20
405	7.7656E+15	465	4.5726E+18	525	9.6713E+20
407	1.1983E+16	467	5.4691E+18	527	1.1557E+21
409	1.7027E+16	469	6.5408E+18	529	1.3812E+21
411	2.3058E+16	471	7.8218E+18	531	1.6506E+21
413	3.0269E+16	473	9.3531E+18	533	1.9725E+21
415	3.8893E+16	475	1.1183E+19	535	2.3571E+21
417	4.9204E+16	477	1.3371E+19	537	2.8168E+21
419	6.1532E+16	479	1.5986E+19	539	3.3660E+21
421	7.6274E+16	481	1.9112E+19	541	4.0223E+21
423	9.3900E+16	483	2.2849E+19	543	4.8064E+21
425	1.1497E+17	485	2.7315E+19	545	5.7434E+21
427	1.4017E+17	487	3.2654E+19	547	6.8629E+21
429	1.7030E+17	489	3.9035E+19	549	8.2005E+21
431	2.0632E+17	491	4.6661E+19	551	9.7988E+21
433	2.4939E+17	493	5.5777E+19	553	1.1708E+22
435	3.0089E+17	495	6.6672E+19	555	1.3989E+22
437	3.6245E+17	497	7.9693E+19	557	1.6715E+22
439	4.3606E+17	499	9.5257E+19	559	1.9972E+22
441	5.2407E+17	501	1.1385E+20	561	2.3863E+22
443	6.2928E+17	503	1.3608E+20	563	2.8512E+22
445	7.5507E+17	505	1.6265E+20	565	3.4066E+22
447	9.0545E+17	507	1.9441E+20	567	4.0702E+22
449	1.0852E+18	509	2.3236E+20	569	4.8629E+22
451	1.3001E+18	511	2.7771E+20	571	5.8100E+22
453	1.5571E+18	513	3.3191E+20	573	6.9414E+22
455	1.8643E+18	515	3.9668E+20	575	8.2930E+22
457	2.2315E+18	517	4.7409E+20		
459	2.6705E+18	519	5.6660E+20		

(1.0000E+05 = 1.0000×10^5)

where

$$I_{ps} \equiv \int_{T_{ss}}^{T_{es}} A(T)^{\frac{1}{m}}\,E(T)^{\frac{\gamma}{m}}\,dT\,, \quad T_{ss} = 400\ (°C)$$

Table 1 Calculated result of the integration of the left hand side of Eq. (1)

T_{ep}	I_{pp}	T_{ep}	I_{pp}	T_{ep}	I_{pp}
577	2.8825E+09	619	2.5238E+11	661	2.3693E+12
579	6.1080E+09	621	2.8373E+11	663	2.6128E+12
581	9.7162E+09	623	3.1848E+11	665	2.8793E+12
583	1.3751E+10	625	3.5701E+11	667	3.1706E+12
585	1.8261E+10	627	3.9970E+11	669	3.4888E+12
587	2.3302E+10	629	4.4696E+11	671	3.8362E+12
589	2.8932E+10	631	4.9927E+11	673	4.2149E+12
591	3.5219E+10	633	5.5713E+11	675	4.6276E+12
593	4.2237E+10	635	6.2109E+11	677	5.0767E+12
595	5.0068E+10	637	6.9175E+11	679	5.5651E+12
597	5.8803E+10	639	7.6978E+11	681	6.0957E+12
599	6.8542E+10	641	8.5588E+11	683	6.6714E+12
601	7.9396E+10	643	9.5084E+11	685	7.2955E+12
603	9.1488E+10	645	1.0555E+12	687	7.9712E+12
605	1.0495E+11	647	1.1707E+12	689	8.7021E+12
607	1.1994E+11	649	1.2976E+12	691	9.4917E+12
609	1.3662E+11	651	1.4372E+12	693	1.0343E+13
611	1.5516E+11	653	1.5906E+12	695	1.1261E+13
613	1.7578E+11	655	1.7591E+12	697	1.2250E+13
615	1.9869E+11	657	1.9441E+12	699	1.3312E+13
617	2.2414E+11	659	2.1470E+12	700	1.3872E+13

(1.0000E+05 = 1.0000×10^5)

where

$$I_{pp} \equiv \int_{T_{sp}}^{T_{ep}} \beta(T)\,E(T)^n\,dT\,, \quad T_{sp} = 575\ (°C)$$

Table 2 Calculated result of the integration of the left hand side of Eq. (3)

${}_n\varepsilon^e_{x1}$	$-I_s$	${}_n\varepsilon^e_{x1}$	$-I_s$	${}_n\varepsilon^e_{x1}$	$-I_s$
0.99	1.3052E-06	0.66	5.6983E-01	0.33	1.7724E+03
0.98	9.4448E-06	0.65	7.0337E-01	0.32	2.4468E+03
0.97	3.1066E-05	0.64	8.6831E-01	0.31	3.4077E+03
0.96	7.4075E-05	0.63	1.0722E+00	0.30	4.7908E+03
0.95	1.4816E-04	0.62	1.3248E+00	0.29	6.8035E+03
0.94	2.6531E-04	0.61	1.6379E+00	0.28	9.7670E+03
0.93	4.4032E-04	0.60	2.0269E+00	0.27	1.4186E+04
0.92	6.9147E-04	0.59	2.5108E+00	0.26	2.0866E+04
0.91	1.0413E-03	0.58	3.1141E+00	0.25	3.1112E+04
0.90	1.5175E-03	0.57	3.8676E+00	0.24	4.7083E+04
0.89	2.1543E-03	0.56	4.8110E+00	0.23	7.2408E+04
0.88	2.9936E-03	0.55	5.9948E+00	0.22	1.1333E+05
0.87	4.0866E-03	0.54	7.4841E+00	0.21	1.8083E+05
0.86	5.4963E-03	0.53	9.3628E+00	0.20	2.9472E+05
0.85	7.2996E-03	0.52	1.1739E+01	0.19	4.9173E+05
0.84	9.5908E-03	0.51	1.4755E+01	0.18	8.4202E+05
0.83	1.2485E-02	0.50	1.8594E+01	0.17	1.4843E+06
0.82	1.6123E-02	0.49	2.3498E+01	0.16	2.7032E+06
0.81	2.0678E-02	0.48	2.9786E+01	0.15	5.1080E+06
0.80	2.6359E-02	0.47	3.7877E+01	0.14	1.0065E+07
0.79	3.3427E-02	0.46	4.8331E+01	0.13	2.0817E+07
0.78	4.2195E-02	0.45	6.1897E+01	0.12	4.5534E+07
0.77	5.3052E-02	0.44	7.9579E+01	0.11	1.0638E+08
0.76	6.6473E-02	0.43	1.0273E+02	0.10	2.6885E+08
0.75	8.3040E-02	0.42	1.3321E+02	0.09	7.4728E+08
0.74	1.0346E-01	0.41	1.7354E+02	0.08	2.3365E+09
0.73	1.2864E-01	0.40	2.2721E+02	0.07	8.4822E+09
0.72	1.5963E-01	0.39	2.9905E+02	0.06	3.7443E+10
0.71	1.9780E-01	0.38	3.9581E+02	0.05	2.1593E+11
0.70	2.4478E-01	0.37	5.2701E+02	0.04	1.8345E+12
0.69	3.0262E-01	0.36	7.0617E+02	0.03	2.8760E+13
0.68	3.7385E-01	0.35	9.5264E+02	0.02	1.3795E+15
0.67	4.6162E-01	0.34	1.2944E+03	0.01	1.0164E+18

(1.0000E+05 = 1.0000×10^5)

where

$$I_s \equiv \int_1^{{}_n\varepsilon^e_{x1}} ({}_n\varepsilon^e_{x1})^{-\frac{\gamma}{m}}\,(1-{}_n\varepsilon^e_{x1})^{\frac{1}{m}-1}\,d_n\varepsilon^e_{x1}$$

Table 3 Calculated result of the integration of the right hand side of Eq. (1)

The influence of coefficient b_1 on the stress change is small in the welded joint in stress self-balance. However, in this study, two values are set up for coefficient b_1 to consider the influence. Two values are 1 and 2. The actual value of b_1 is thought to be between them (Refer to Table 4 in the third report). In the case of $b_1=1$, somewhat smaller stress is estimated than the actual magnitude because the influence of b_1 is ignored. In the case of $b_1=2$, conversely a somewhat larger stress is estimated. In the next chapter, the stress change during SR treatment will be estimated for these two cases.

4. Application of Estimation Method and Its Accuracy

Applicability of the simple estimation method developed in the third report is examined as follows.

4.1 Estimated Results

In the second report, the stress change during SR treatment in the butt welded joint of thick plate was accurately analyzed by the finite element method. Here, the stress change is calculated by the simple estimation method, and the results are compared with the ones by the finite element method.

The positions where the stress change is estimated are two, positions A and B shown in Fig. 3 and Fig. 4. At the position A, the maximum tensile stress σ_x is produced in the whole specimen, and, at the position B, the maximum one on the surface is found. Particular attention has to be paid to these positions from the viewpoint of stresses for SR cracking and cold cracking.

The calculated results with the simple method, that is, the stress changes at each position during SR treatment are shown in **Figs. 6 and 7,** for two restraint conditions, . Only the change of σ_x which is maximum stress component is shown in the figures. In this estimation method, it is assumed that the stress component ratio in the welding residual stresses does not change during SR treatment. Accordingly, the other stress components are considered to decrease in the same ratio to σ_x.

○ mark and ▽ mark show the values estimated in multi-axial stress state. ○ mark is in the case assuming coefficient $b_1=1$, and ▽ mark is in the case of $b_1=2$. △ mark is the result under the assumption of the uni-axial stress state (that is, the stress components except σ_x are 0) and coefficient $b_1=1$. In other words, it represents the case where relaxation tests at changing and constant temperatures are done, setting the welding residual stress σ_x as the initial stress value.

In Figs.6(a) and 7(a), for the stress change of the position A at the middle cross-section, ○ mark, corresponds with the result by the finite element method, very well. The estimated value △ under the condition as the relaxation test has enough accuracy, too.

On the other hand, for the stress change of the position B (the toe of weld), ○ mark shows high accuracy until 575 °C, as seen in Figs. 6(b) and 7(b). When the temperature becomes higher and the stress becomes small, ▽ mark gives good approximate value.

4.2 Characteristics of Stress Reduction during SR Treatment

The above-mentioned results can be explained as follows. At the position where the stresses are large, the reduction rates of the stresses are dependent mainly on the values of themselves and the initial ratio of them, in the early period. Even if the stress component ratio changes (even if coefficients S_1 - S_6 change), the influence is small. And, even if the surroundings displace due to the changes in the stresses (even if coefficients b_1 and b_2 change), the influence is small, too. Accordingly, until 575 °C, the ○ mark corresponds well with the result by the finite element method at both position A and position B.

When the temperature becomes higher, and the stress decreases largely, the difference of the value among the stress components becomes small. The difference from the surroundings becomes small, too. These changes make the behavior rather more complex. As a result, at the toe of weld, the actual stresses predicted by the finite element method are somewhat hard to decrease, compared with the estimated values. But, the difference between ○ mark and FEM is only about 1 kgf/mm^2. The ▽ mark shows the best approximate value in this situation. In the whole period of the stress reduction during SR treatment, the estimation method has high accuracy.

From the above-mentioned results, the following conclusion can be obtained. In the case of a welded joint where the stresses are in self-balance, the influence of the stress change of the surroundings is small (coefficient b_1 has little effect). For the change of the maximum stress, the influence of multi-axial stress state is comparatively small, too. But, to estimate the stress change during SR treatment, erring on the safety side, the calculation should be conducted as follows. The coefficients C_{ss} and C_{ps} are calculated from the initial stress and strain state. The coefficients C_{sb} and C_{pb} are obtained as coefficient $b_1=2$. On the other hand, if it is replaced in the relaxation test (uni-axial stress state and $b_1=1$), the estimated value is not so bad, and may be only a little smaller than the actual one.

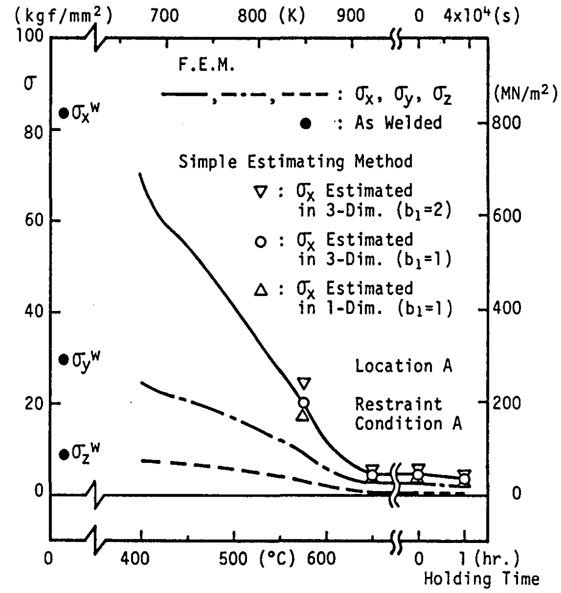

(a) Change of the largest welding residual stress σ_x

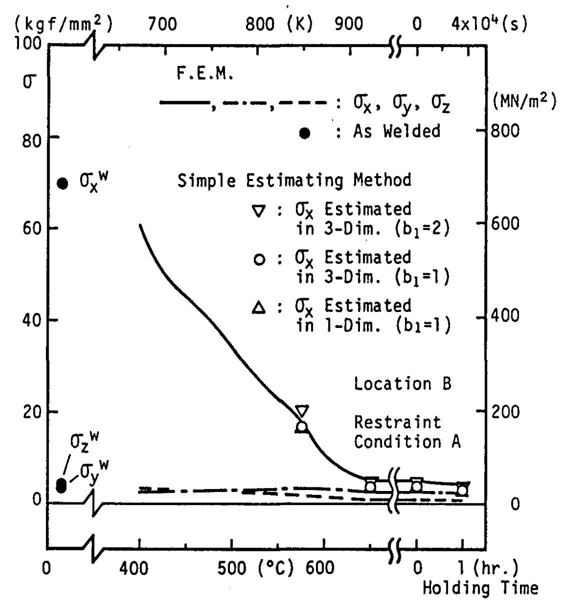

(b) Change of the welding residual stress σ_x at toe of weld

Fig. 6 Estimated results of change of welding residual stress during SR (In the case of restraint condition A)

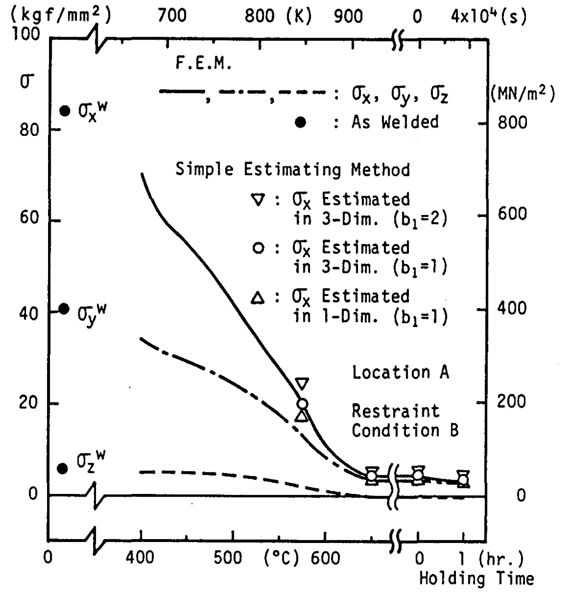

(a) Change of the largest welding residual stress σ_x

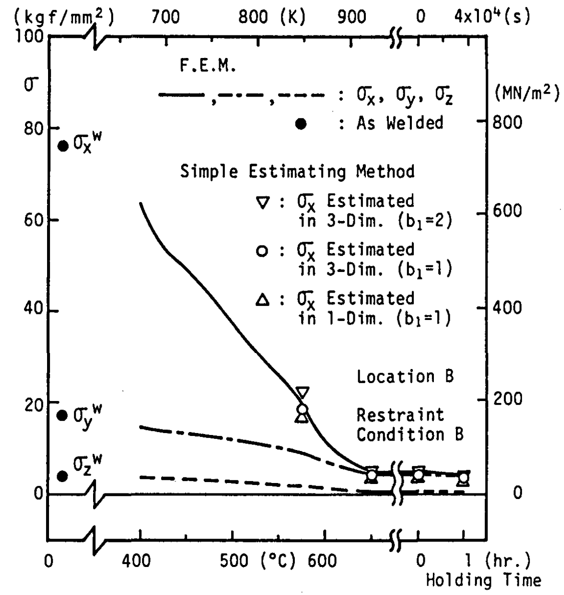

(b) Change of the welding residual stress σ_x at toe of weld

Fig. 7 Estimated results of change of welding residual stress during SR (In the case of restraint condition B)

5. Conclusion

In this serial study, a simple analytical method (as simple as hand calculation) was developed, which can obtain the stress change during SR treatment in thick welded joints. The results from the first report to this fourth report are summarized as follows.

1) In the first report, approximate estimation equations for relaxation tests were developed.

2) In the second report, the characteristics of the stress change during SR treatment of thick welded joints were studied by the analyses with the finite element method.

3) In the third report, the approximate estimation equations developed in the first report were expanded for multi-axial stress state, based on the above characteristics.

4) In the fourth report, applicability of the estimation

equations was examined for the SR treatment of thick welded joints, which was analyzed in the second report. As a result, it was confirmed that this analytical method has enough accuracy for practical use.

In the application of this estimation method, the following calculations are useful. For example, the influence of the initial stress state on the stress reduction rate during SR treatment can be estimated systematically, using the values of coefficients C_s and C_p calculated for various initial stress states. Then the characteristics of their relation can be studied. Next, the quantity of the creep strain is regarded as an important mechanical factor, like the magnitude of stress, for the occurrence of SR cracking. The quantity of the creep strain can be estimated by two equations shown in the third report, that is, the first equation in Eq. (9) and the third equation in Eq. (8). In that case, the influence of coefficient b_1 becomes large. These studies will be described in other papers.

Acknowledgement

The authors would like to thank Mr. H. Morikawa, Kobe Steel, Ltd. (formerly, a student of Osaka University), and Mr. M. Yoshikawa, Toyota Motor Corp. (formerly, a student of Osaka University), for their helpful assistance in this research.

References

1) Y. Ueda and K. Fukuda : Application of finite element method for Analysis on Process of Stress Relief Annealing, Trans. of JWRI, Vol.4(1975), No.1, pp.39-45, and J. of JWS (The Japan Welding Society), Vol.44(1975), No.11, pp.902-908 (in Japanese), and Trans. of JWS, Vol.8(1977), No.1, pp.19-25.
2) Y. Ueda, E. Takahashi, K. Fukuda, K. Sakamoto and K. Nakacho : Multipass Welding Stresses in Very Thick Plates and Their Reduction from Stress Relief Annealing, Trans. of JWRI, Vol.5(1976), No.2, pp.179-189, and ASME, Proc. of Third Int. Conf. on Pressure Vessel Technology (1977), PartII, pp.925-933, and J. of JWS, Vol.47(1978), No.8, pp.500-506 (in Japanese).
3) K. Nakacho and Y. Ueda : An Efficient Method for Estimation of Reduction of Welding Residual Stresses from Stress-Relief Annealing (Report I) - Development of Basic Equations for One-dimensional Stress State and Their Accuracy -, Quarterly J. of JWS, Vol.1(1983), No.2, pp.174-181 (in Japanese), and Trans. of JWRI, Vol.16 (1987), No.2, pp.131-138.
4) K. Nakacho and Y. Ueda : An Efficient Method for Estimation of Reduction of Welding Residual Stresses from Stress-Relief Annealing (Report II) - The characteristics of Reduction of Welding Residual Stresses in Very Thick Joints during SR treatment -, Quarterly J. of JWS, Vol.6 (1988), No.1, pp.151-158 (in Japanese), and Trans. of JWRI, Vol.23(1994), No.1, pp.79-84.
5) K. Nakacho and Y. Ueda : An Efficient Method for Estimation of Reduction of Welding Residual Stresses from Stress-Relief Annealing (Report III) - Development of Estimation Equations for Multi-Axial Stress State in Thick Welded Joint -, Quarterly J. of JWS, Vol.6(1988), No.1, pp.151-158 (in Japanese), and Trans. of JWRI, Vol.24 (1995), No.1, pp.113-120.